Ordered and Disordered Aspects of Interlayer Guests in Superconducting Hydrous Sodium Cobalt Oxides

Kazunori Takada,*[,†,§] Mitsuko Onoda,[†] Dimitri N. Argyriou,[‡] Yong-Nam Choi,[||] Fujio Izumi,[†] Hiroya Sakurai,[†] Eiji Takayama-Muromachi,[†] and Takayoshi Sasaki[†,§]

National Institute for Materials Science, 1-1 Namiki, Tsukuba, Ibaraki 305-0044, Japan, Hahn-Meitner-Institut, Glienicker Strasse 100, Berlin D-14109, Germany, Korea Atomic Energy Research Institute, 150 Deokjin-dong, Yuseong-gu, Daejeon 305-353, Korea, and Japan Science and Technology Agency, 4-1-8, Honcho, Kawaguchi, Saitama 332-0012, Japan

Received February 27, 2007. Revised Manuscript Received April 24, 2007

Crystal structures of two kinds of cobalt oxide superconductors were investigated by neutron powder diffraction. Comparison between the structures of the two phases, one derived from γ-$Na_{0.7}CoO_2$ and the other from α-$NaCoO_2$, indicated that the guest arrangement is common to the two phases in spite of the difference in stacking made of CoO_2 host layers. Structure analysis on the basis of composite crystal models with stacking faults revealed that the hydrated sodium ions in the galleries are ordered to form a $2/\sqrt{3}a \times 2/\sqrt{3}a$ trigonal lattice, where a is a lattice constant of the fundamental unit cell. The guest layers were found to be stacked along the c-direction with a short-range interlayer ordering: when a guest layer is stacked onto another over a CoO_2 layer interposed between them, the stacking must be accompanied by a lateral shift with shift vectors, $1/2\boldsymbol{a}_2$, $1/2\boldsymbol{b}_2$, and $1/2\boldsymbol{a}_2 + 1/2\ \boldsymbol{b}_2$, where $\boldsymbol{a}_2$ and $\boldsymbol{b}_2$ are lattice vectors of the $2/\sqrt{3}a \times 2/\sqrt{3}a$ lattice with the same probability.

Introduction

The discovery of a superconducting sodium cobalt oxide[1] has triggered intensive investigations on its superconducting mechanism. Hundreds of papers have been published, and various theoretical and experimental information has been provided. However, the accurate crystal structure, which is essential for the studies on the superconductor, has not been understood in full detail yet. Particularly, little is known about the precise arrangement of the interlayer guests, because they are highly disordered in the arrangement and hardly seen in X-ray diffraction. Because D and O nuclei have large scattering amplitude for neutrons, neutron diffraction (ND) should yield much information on the arrangement of the guests. However, the highly disordered arrangement still conceals the accurate structure.

The most prominent feature observed in the ND patterns was strong bands at $d = 2.8$ and 2.6 Å. They were not indexable on the fundamental hexagonal host lattice and were wider in the profile width than the other reflections; therefore, they were at first attributed to impurity phases.[2] However, they were observed with good reproducibility in the samples synthesized in different laboratories,[3] which strongly suggested that the two bands should be an intrinsic structural feature. Jorgensen et al. attributed them to superposed $30l$ Bragg reflections from an orthorhombic supercell with dimensions of $3a \times \sqrt{3}a \times 3c$;[3a] however, the crystal structure was analyzed only on the basis of the fundamental lattice. On the other hand, a double hexagonal supercell with dimensions of $2a \times 2a \times c$ was proposed to take into account the first band in the structure refinement.[3b] The structure model reproduced the first band but not the second one. In short, no paper has ever consistently explained the origin of the two bands.

The first cobalt oxide superconductor, for which the above-mentioned ND studies were done, was synthesized from γ-$Na_{0.7}CoO_2$ and has a hexagonal lattice involving two-layer periodicity of the CoO_2 layers (2H type). More recently, another superconducting hydrate was derived from α-$NaCoO_2$,[4] which has a rhombohedral lattice with three-layer periodicity (3R type). It has CoO_2 layers identical to those in the 2H phase and the same interlayer distance of 9.8 Å; however, the stacking sequence is different. In this paper, ND patterns for the two phases are analyzed in order to clarify how the guests are arranged in the galleries.

Experimental Section

Superconducting samples with the 2H and 3R structures used for the neutron powder diffraction experiments were synthesized

* Corresponding author. E-mail: takada.kazunori@nims.go.jp.
† National Institute for Materials Science.
‡ Hahn-Meitner-Institut.
|| Korea Atomic Energy Research Institute.
§ Japan Science and Technology Agency.

(1) Takada, K.; Sakurai, H.; Takayama-Muromachi, E.; Izumi, F.; Dilanian, R. A.; Sasaki, T. *Nature* **2003**, *422*, 53.
(2) Lynn, J. W.; Huang, Q.; Brown, C. M.; Miller, V. L.; Foo, M. L.; Schaak, R. E.; Jones, C. Y.; Mackey, E. A.; Cava, R. J. *Phys. Rev.* **2003**, *B68*, 214516.
(3) (a) Jorgensen, J. D.; Avdeev, M.; Hinks, D. G.; Burley, J. C.; Short, S. *Phys. Rev.* **2003**, *B68*, 214517. (b) Argyriou, D. N.; Radaelli, P. G.; Milne, C. J.; Aliouane, N.; Chapon, L. C.; Chemseddine, A.; Veira, J.; Cox, S.; Mathur, N. D.; Midgley, P. A. *J. Phys. Condens. Matter* **2005**, *17*, 3293.
(4) (a) Takada, K.; Sakurai, H.; Takayama-Muromachi, E.; Izumi, F.; Dilanian, R. A.; Sasaki, T. *Adv. Mater.* **2004**, *16*, 1901. (b) Foo, M. L.; Klimczuk, T.; Li, L.; Ong, N. P.; Cava, R. J. *Solid State Commun.* **2005**, *133*, 407.

10.1021/cm0705441 CCC: $37.00
Published on Web 06/09/2007

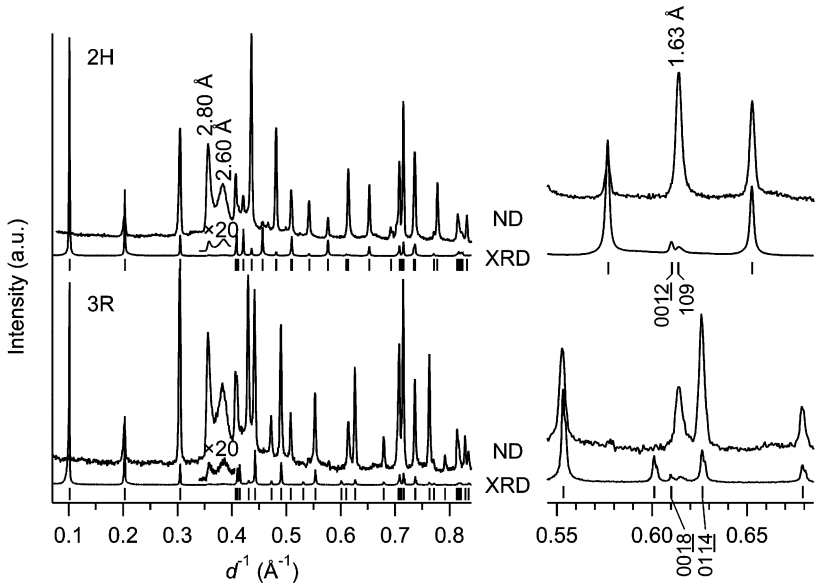

Figure 1. XRD and ND patterns for the 2H (upper) and 3R (lower) phases. The XRD intensities between $d^{-1} = 0.34$ Å^{-1} and $d^{-1} = 0.40$ Å^{-1} were multiplied by 20 to make the plots easier to read. Short bars below the patterns indicate the positions of allowed Bragg reflections from the 2H and 3R lattices. The right panel is an expansion around $d = 1.63$ Å.

according to the procedures previously reported[1,4a] except for the use of D_2O in place of H_2O. The compositions were determined by the following chemical analyses. Because the cobalt oxides accommodate protons or oxonium ions as well as Na^+ ions and H_2O molecules in the interlayers,[5] the compositions of the deuterated samples were assumed to be $Na_x(D_2O)_yD_zCoO_2$. The Na and Co contents were measured by inductively coupled plasma atomic emission spectrometry (ICP-AES) to determine x, and the oxidation states of Co, V(Co), were determined by redox titration in order to calculate z by the equation of $4 - x - z = V(\mathrm{Co})$. The D_2O content, y, was deduced by attributing the residual mass calculated from the x and z to the D_2O molecules. It was confirmed that the chemical compositions obtained by this way were consistent with the results from thermogravimetry−mass spectroscopy (TG−MS).

The ND for the 2H phase was taken on a high-resolution powder diffractometer at HANARO in the Korean Atomic Energy Center; the wavelength of the neutron beam was 1.8346 Å. Meanwhile, the ND pattern for the 3R phase was collected at the Berlin Neutron Scattering Center of the Hahn-Heitner-Institut at a wavelength of 1.797 Å.

Their powder diffraction patterns were simulated on the basis of a composite crystal model[6] by a matrix method[7] and fitted to the observed ones. The crystal structures were separated into host and guest subsystems, and the diffraction intensities were calculated by a computer program, FU1,[8] by the matrix method. Another program, PPROF,[9] was modified in order to merge the diffractions from the two subsystems by taking into account the misfit between the two-dimensional lattices and different unit cell volumes of the subsystems and convert them into powder patterns. The simulated patterns were fitted to the observed ones by a least-squares method.

In the structure analysis, the Na and D_2O contents were fixed to those obtained by the above chemical analyses. Note that all the D_2O molecules in the samples could be assigned as the interlayer hydration water. If the samples contain a considerable amount of adsorbed water present at particle surface and intergrain region, it should freeze into ice and give additional reflections at low temperature; three strong lines should be located at $d^{-1} = 0.255$, 0.272, and 0.290 Å^{-1} as reported in ref 2. They were not observed in the diffraction patterns taken at 2 K for the present samples, as shown in Figure S1 in Supporting Information.

Results and Discussion

Intralayer Ordering of the Guests. The ND patterns for the deuterated 2H and 3R superconductors are shown in Figure 1 in comparison with the XRD patterns for the corresponding samples hydrated with H_2O.[4a,5] The diffuse bands at $d = 2.80$ and 2.60 Å ($d^{-1} = 0.357$ and 0.384 Å^{-1}, respectively), which were reported in the previous papers, were also observed for the present 2H sample. The two bands were extremely weak and hardly seen in the XRD pattern but pronounced in the ND one, which strongly suggests that the guests including D_2O molecules with large scattering amplitudes are responsible for the two bands. Thus the analysis of the two bands should help clarify the guest accommodation structure. More surprisingly, the 3R phase also gave a similar diffuse pattern with the two bands at the same d-spacings in spite of its different fundamental lattice.

The two bands are not indexable on the basis of the 2H and 3R lattices for the host frameworks (space groups: $P6_3/mmc$ and $R\bar{3}m$, respectively). In addition, the 3R phase clearly gave another reflection at $d = 1.63$ Å that was not indexed; this was also observed for the 2H phase, but is misleading because of the reason described below. The reflections were also very weak in the XRD patterns but pronounced in the ND ones, which again strongly suggests that both of them originated from the guests. The two d-spacings of 2.80 and 1.63 Å are close to those of 10 and 11 in-plane reflections from a trigonal sheet with dimensions of $2/\sqrt{3}a \times 2/\sqrt{3}a$,

(5) Takada, K.; Fukuda, K.; Osada, M.; Nakai, I.; Izumi, F.; Dilanian, R. A.; Kato, K.; Takata, M.; Sakurai, H.; Takayama-Muromachi, E.; Sasaki, T. *J. Mater. Chem.* **2004**, *14*, 1448.
(6) Janner, A.; Janssen, T. *Acta Crystallogr., Sect. A* **1980**, *36*, 408.
(7) (a) Hendricks, S.; Teller, E. *J. Chem. Phys.* **1942**, *10*, 147. (b) Kakinoki, J.; Komura, Y. *Acta. Crystallogr.* **1965**, *19*, 137. (c) Kakinoki, J. *Acta Crystallogr.* **1967**, *23*, 875.
(8) Kato, K.; Kosuda, K.; Toga, T.; Nagasawa, H. *Acta Crystallogr., Sect. C* **1990**, *46*, 1587.
(9) Onoda, M.; Saseki, M.; Kawada, I. *Acta Crystallogr., Sect. A* **1980**, *36*, 952.

suggesting that the guests are ordered in the galleries to form the trigonal lattice. The broad band at $d = 2.60$ Å may be caused by a frequently observed feature in layered systems with stacking faults. It should be noted that no paper has paid attention to the reflection at $d = 1.63$ Å in the 2H phase, for which all the crystal structure studies so far have focused on. For the 2H phase, the reflection has been assigned as the 109 reflection of the fundamental cell because of its very close location as shown in the figure. However, the reflection in the XRD pattern was broader than the others and similar in the profile to that observed for the 3R phase, which supports the idea that the reflection in the ND pattern should be the 11 in-plane reflection from the guest layer rather than the Bragg reflection from the 2H host lattice.

In summary, the remarkable features observed in the ND are the diffuse band at 2.80 Å followed by the hump at 2.60 Å and the reflection at 1.63 Å, which are common to the 2H and 3R phases. The similarities in the profiles and the *d*-spacings suggest that the guests have the same arrangements with the intralayer ordering in the two phases in spite of their different stacking sequences of the CoO_2 host layers.

Composite Crystal Model for Structural Analysis. The CoO_2 layers form a trigonal sheet with periodic dimensions of $a \times a$, whereas the guests are arranged in a $2/\sqrt{3}a \times 2/\sqrt{3}a$ two-dimensional lattice. The 2H and 3R phases have different stacking sequences of the CoO_2 layers; however, the arrangements of the guests are common to the two phases. In addition, the structural studies based on the XRD[4a,5] indicate that the CoO_2 layers have regular stacking, whereas the diffuse patterns in the ND patterns suggest that the stacking of the guest layers is disordered. Therefore, the crystal structures were analyzed on the basis of composite crystal models, in which the crystal structures were separated into two subsystems of the CoO_2 host layers and guest layers; the host subsystems are different between the two phases, whereas the guest subsystem is common.

A structure model for the host layer was constructed as follows. The 2H and 3R phases are built from identical CoO_2 layers with the same interlayer distance of 9.8 Å, and unit cells for the 2H and 3R phases contain two and three CoO_2 layers, respectively. Therefore, lattice vectors for the host subsystem, $\boldsymbol{a}_1$, $\boldsymbol{b}_1$, and $\boldsymbol{c}_c$, were chosen in such a way that $\boldsymbol{a}_1 = \boldsymbol{a}_{2H} = \boldsymbol{a}_{3R}$, $\boldsymbol{b}_1 = \boldsymbol{b}_{2H} = \boldsymbol{b}_{3R}$, and $\boldsymbol{c}_c = 1/2\boldsymbol{c}_{2H} = 1/3\boldsymbol{c}_{3R}$, where $\boldsymbol{a}_{2H}$, $\boldsymbol{b}_{2H}$, and $\boldsymbol{c}_{2H}$ are the lattice vectors for the 2H phase, whereas $\boldsymbol{a}_{3R}$, $\boldsymbol{b}_{3R}$, and $\boldsymbol{c}_{3R}$ are those for the 3R phase.

On the other hand, the guests should be ordered to form a $2/\sqrt{3}a \times 2/\sqrt{3}a$ lattice. The interlayer distance in the guest subsystem is, again, 9.8 Å. Therefore, lattice vectors for the guest layer were set to be $\boldsymbol{a}_2 = 2/3\boldsymbol{a}_1 + 4/3\boldsymbol{b}_1$, $\boldsymbol{b}_2 = -4/3\boldsymbol{a}_1 - 2/3\boldsymbol{b}_1$, and $\boldsymbol{c}_c$, as shown in Figure 2a.

Structure models for the basic host and guest layers are illustrated in panels a and b of Figure 2. Co and O atoms are arranged in the cell of $\boldsymbol{a}_1 \times \boldsymbol{b}_1 \times \boldsymbol{c}_c$ on the basis of the structure parameters refined from the XRD data.[4a,5] On the other hand, the previous XRD studies do not provide a reliable guest arrangement structure. Because the lattice symmetries were determined from the Bragg reflections originating from the different host sublattices, different space groups, $P6_3/mmc$ and $R\bar{3}m$, were assigned to the 2H and 3R

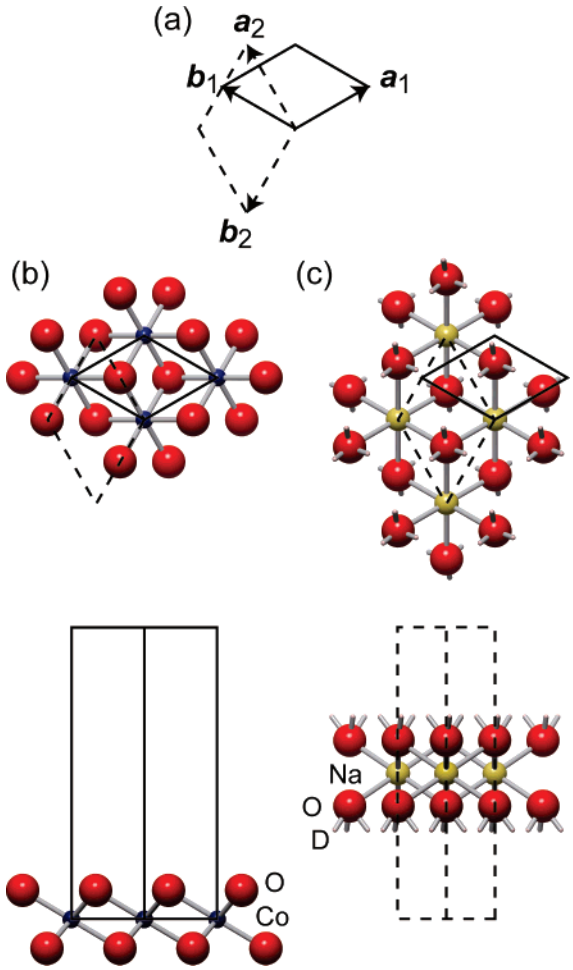

Figure 2. (a) Trigonal lattices for the host (solid line) and guest (broken line) basic layers, and structure models for the basic (b) host and (c) guest layers.

phases, respectively. Hence the guest arrangements were refined to be different between the two phases as well. In the 2H phase with $P6_3/mmc$ symmetry, Na^+ ions are situated on sixfold inversion axes, and the symmetry operation results in trigonal prismatic coordination of D_2O molecules around the Na^+ ions. On the other hand, they lie on threefold inversion axes in the 3R phase, which leads to octahedral coordination. That is, the structure refinements for the 2H and 3R phases from the XRD data resulted in the different coordinations around the Na^+ ions, respectively. However, the comparison between the ND patterns for the 2H and 3R phases revealed that the guest arrangements are common to the two phases, and thus the coordination must be the same as well. We tested both of the coordination environments and found that the octahedral coordination gives much better fitting results than the trigonal prismatic one. Therefore, the structure model for the basic guest layer is constructed as shown in Figure 2c, in which Na^+ ions are octahedrally coordinated with D_2O molecules, and the octahedra share their edges to form a trigonal guest layer.

The host and guest layers were stacked to construct the corresponding subsystems, respectively. The CoO_2 basic layers should be stacked in a regular way to give Bragg reflections in the XRD patterns. On the other hand, the diffuse bands pronounced in the ND patterns are evidence for the disordered stacking of the guest layers along the *c*

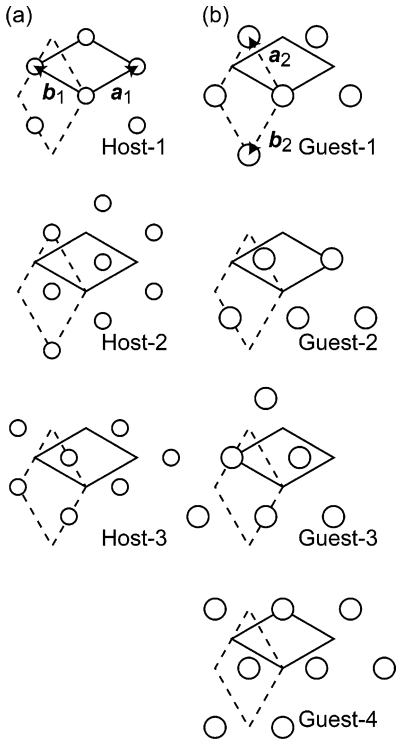

Figure 3. Host and guest layers in the subsystems. Circles in (a) and (b) indicate the positions of Co and Na atoms in the host and guest layers, respectively.

Table 1. P Table for the Host Subsystem in the 3R Phase

i-th/(*i*+1)-th	host-1	host-2	host-3
host-1	0	1	0
host-2	0	0	1
host-3	1	0	0

direction. The diffraction patterns from the subsystems were simulated by the matrix method in order to take into account the irregular stacking, or stacking faults. In the matrix method, the stacking is represented by a probability table (P table), in which *p*(layer-*m*, layer-*n*) denoting the probability that layer-*n* is stacked onto layer-*m* is tabulated. First, the structure model for the 3R phase is constructed as described below.

In the 3R phase, the CoO_2 layers have regular stacking to form a rhombohedral lattice. The host basic layer is stacked on another with a unique shift vector of $2/3\boldsymbol{a}_1 + 1/3\boldsymbol{b}_1 + \boldsymbol{c}_c$. In other words, when the three kinds of CoO_2 layers, host-1, host-2, and host-3, are generated by shift vectors $(0, 2/3\boldsymbol{a}_1 + 1/3\boldsymbol{b}_1, 1/3\boldsymbol{a}_1 + 2/3\boldsymbol{b}_1)$ as shown in Figure 3a, they were stacked in the order of host-1−host-2−host-3−host-1−... with a shift vector of $\boldsymbol{c}_c$ to form the rhombohedral lattice. The stacking can be represented by the probability matrix shown in Table 1.

Because the guest layers also belong to a trigonal lattice, the simplest set of the shift vectors is $\boldsymbol{c}_c$, $2/3\boldsymbol{a}_2 + 1/3\boldsymbol{b}_2 + \boldsymbol{c}_c$, and $1/3\boldsymbol{a}_2 + 2/3\boldsymbol{b}_2 + \boldsymbol{c}_c$. However, the simulated patterns based on the structure model did not fit to the observed ones, as shown in Figures S2 and S3 in Supporting Information. Therefore, the next simplest model with four possible configurations shown in Figure 3b was adopted for the guest subsystem, which were generated from the guest basic layer by shift vectors of $\boldsymbol{0}$, $1/2\boldsymbol{a}_2$, $1/2\boldsymbol{b}_2$, and $1/2\boldsymbol{a}_2 + 1/2\boldsymbol{b}_2$. The

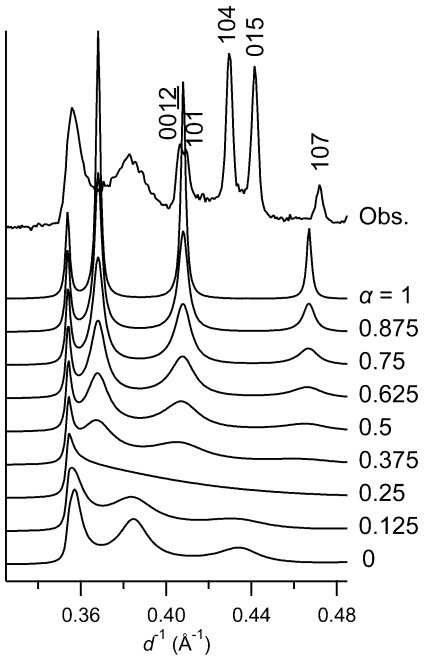

Figure 4. Diffuse patterns simulated with different α. The observed ND pattern is drawn on the top, with Miller indexes on the rhombohedral host lattice indicated.

Table 2. P Table for the Guest Subsystem in the 3R Phase

i-th/(*i*+1)-th	guest-1	guest-2	guest-3	guest-4
guest-1	α	(1 − α)/3	(1 − α)/3	(1 − α)/3
guest-2	(1 − α)/3	α	(1 − α)/3	(1 − α)/3
guest-3	(1 − α)/3	(1 − α)/3	α	(1 − α)/3
guest-4	(1 − α)/3	(1 − α)/3	(1 − α)/3	α

guest layers have the disordered, or irregular stacking; therefore, the (*i* +1)th guest layer stacked on the *i*-th one is not unique; different kinds of the guest layers can be stacked. Such a situation can be represented as plural finite matrix elements in a row in the P table. In Table 2, *p*(guest-*m*, guest-*m*) is set to be different from the others, and the other three are the same. That is, the probability that the same guest layers make a pair over a CoO_2 layer is different from those of the others. Indeed, more complicated models are possible by adopting more shift vectors, assigning different probabilities to different pairs. However, they did not significantly improve the refinement results.

Structure Refinement. The diffuse patterns were simulated for different α. Figure 4 shows the simulated patterns. At α = 1, the guest layers are ordered, and thus the subsystem gives Bragg reflections. With decreasing α, i.e., increasing degree of disorder, the reflections broadened. At α = 1/4, where the guest layers are randomly stacked, the diffuse band had a long tail toward smaller *d*-spacings, which is characteristic of a turbostratic structure. The structure model at α = 0 well-reproduced the two bands at $d = 2.80$ and 2.60 Å. It gave another band at $d = 2.3$ Å ($d^{-1} = 0.43$ Å^{-1}), which was located under the 104 and 015 reflections in the observed pattern. This result indicates that the same guest layers should not make a pair. When a guest layer is stacked onto another interposing a CoO_2 host layer, the stacking should be accompanied by a lateral shift in every direction with the same probability.

The host and guest subsystems were interpenetrated in order to simulate the diffraction pattern. Because the

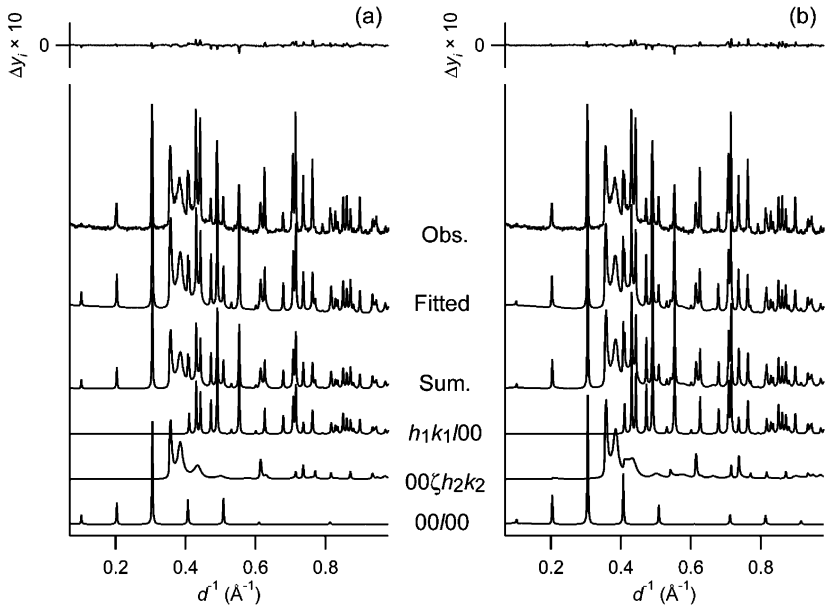

Figure 5. Observed and simulated ND patterns using the basic guest layer with (a) $2/\sqrt{3}a \times 2/\sqrt{3}a$ and (b) $2a \times 2a$ lattices. From the bottom to top, 00l00 basal reflections, $00\zeta h_2k_2$ diffuse patterns, h_1k_1l00 Bragg reflections are displayed. They were summed up to give the total diffraction pattern (the fourth from the bottom) and fitted (the fifth) to the observed one (the sixth). The top curves represent the weighted difference, Δy_i, calculated by $(y_{io} - y_{ic})/\sigma_i$, where y_{io}, y_{ic}, and σ_i are the observed and calculated intensities and the statistical uncertainty of the i-th point, respectively. The differences were multiplied by 10 to make the plots easier to read.

Table 3. Structure Parameters; Fractional Coordinates (*x*, *y*, *z*) and Occupancies (*g*); for the Host and Guest Basic Layers[a]

Host Basic Layer[b]				
atom	x	y	z	*g*
Co	0	0	0	1
O1	1/3	2/3	0.0991(2)	1

Guest Basic Layer[c]				
atom	x	y	z	*g*
Na	0	0	1/2	0.471[d]
O2	2/3	1/3	0.3871(7)	0.893[d]
D	0.586(2)	0.1067(9)	0.3051(3)	0.620(2)

[a] $R_p = 5.58\%$ and $R_{wp} = 8.51\%$. Refined parameters have standard deviations in parentheses. [b] Lattice constants: $a_1 = 2.8239(3)$ Å, $c_c = 9.831(2)$ Å. Symmetry operations: $x, y, z; -y, x-y, z; -x+y, -x, z; -x, -y, -z; y, -x+y, -z; x-y, x, -z$. [c] Lattice constants: $a_2 = a_1 \times 2/\sqrt{3}$, $c_c = 9.831(2)$ Å. Symmetry operations: $x, y, z; -y, x-y, z; -x+y, -x, z; -x, -y, -z; y, -x+y, -z; x-y, x, -z$. [d] These occupancies were fixed to the analyzed values.

interpenetrated structure model has five lattice vectors, $\boldsymbol{a}_1$, $\boldsymbol{b}_1$, $\boldsymbol{c}_c$, $\boldsymbol{a}_2$, and $\boldsymbol{b}_2$, the reflections should be expressed by five indices, $h_1k_1lh_2k_2$. The diffraction patterns were simulated by the fundamental composite crystal model. In the model, h_1k_1l00 ($h_1 \neq 0$ or $k_1 \neq 0$) Bragg reflections and $00\zeta h_2k_2$ ($h_2 \neq 0$ or $k_2 \neq 0$) diffuse bands originating from the host and guest subsystems, respectively, are summed up with 00l00 basal reflections from the interpenetrated system to give a simulated diffraction pattern. The simulated pattern was then fitted to the observed one by the least-square procedure, in which the scale factor and the structure, profile, and background parameters were refined.

Figure 5a shows the simulated and observed patterns, and Table 3 lists the final structure parameters. The above structure model well-reproduced the observed diffuse pattern. However, an appreciable difference was found in the basal reflections; for instance, the 00300 reflection was very weak in the observed ND pattern, whereas it was distinct in the simulated one.

The deviation may be explained by inaccurate coordinates of D atoms. Because the O atoms in the D_2O molecules are on threefold rotation axes in the structure model, the symmetry operation generates three D atoms bonded to the O atom. However, two D atoms are bonded to the O atom with a D−O bond length of ca. 1 Å and a D−O−D bond angle of ca. 108° in an actual D_2O molecule. This discrepancy from the actual structure will be responsible for the unsatisfactory fitting in the basal reflections, because D atoms have large scattering amplitudes in ND. Therefore, the guests in the $2/\sqrt{3}a \times 2/\sqrt{3}a$ lattice were unfolded into a larger lattice in order to lower the symmetry, in which the three equivalent positions for the D atoms in the $2/\sqrt{3}a \times 2/\sqrt{3}a$ lattice become nonequivalent and two D atoms can be positioned around an O atom independently.

It seems reasonable to choose a $2a \times 2a$ lattice as the larger lattice. The D_2O molecules are interposed between the CoO_2 layer and the Na layer; the former forms the $a \times a$ lattice, whereas the latter does the $2/\sqrt{3}a \times 2/\sqrt{3}a$ lattice. Thus the positions and the orientations of the D_2O molecules will be governed by both the lattices. For instance, a D_2O molecule has an electric dipole composed of a negatively charged O atom and positively charged D atoms. The former will be attracted to the Na^+ ions in the $2/\sqrt{3}a \times 2/\sqrt{3}a$ lattice, whereas the latter will be attracted to O atoms in the CoO_2 layer forming the $a \times a$ lattice. Accordingly, a $2a \times 2a$ lattice was used as the larger lattice, because it is divisible by the host lattice as well as the guest lattice.

In the guest subsystem with the $2/\sqrt{3}a \times 2/\sqrt{3}a$ lattice, four guest layers were generated from the basic guest layer by the four shift vectors, $\boldsymbol{s}_i = 0$, $1/2\boldsymbol{a}_2$, $1/2\boldsymbol{b}_2$, and $1/2\boldsymbol{a}_2 + 1/2\boldsymbol{b}_2$. When the $2/\sqrt{3}a \times 2/\sqrt{3}a$ lattice is unfolded into a $2a \times 2a$ lattice, the four shift vectors should be also unfolded

Table 4. Shift Vectors and Guest Layers Generated by the Shift Vectors[a]

s_i	guest layers	s'_{ij}	guest layers
0	guest-1	0,	guest′-11
		$2/3a_3 + 1/3b_3$,	guest′-12
		$1/3a_3 + 2/3b_3$	guest′-13
$1/2a_2$	guest-2	$-1/6a_3 - 1/3b_3$,	guest′-21
		$1/6a_3 + 1/3b_3$,	guest′-22
		$1/2a_3$	guest′-23
$1/2b_2$	guest-3	$1/3a_3 + 1/6b_3$,	guest′-31
		$-1/3a_3 - 1/6b_3$,	guest′-32
		$1/2\ b_3$	guest′-33
$1/2a_2 + 1/2b_2$	guest-4	$1/6a_3 - 1/6b_3$,	guest′-41
		$-1/6a_3 + 1/6b_3$,	guest′-42
		$1/2a_3 + 1/2b_3$	guest′-43

[a] Shift vectors, s_i, are for the $2/\sqrt{3}a \times 2/\sqrt{3}a$ guest lattice and are unfolded into s'_{ij} in the $2a \times 2a$ lattice.

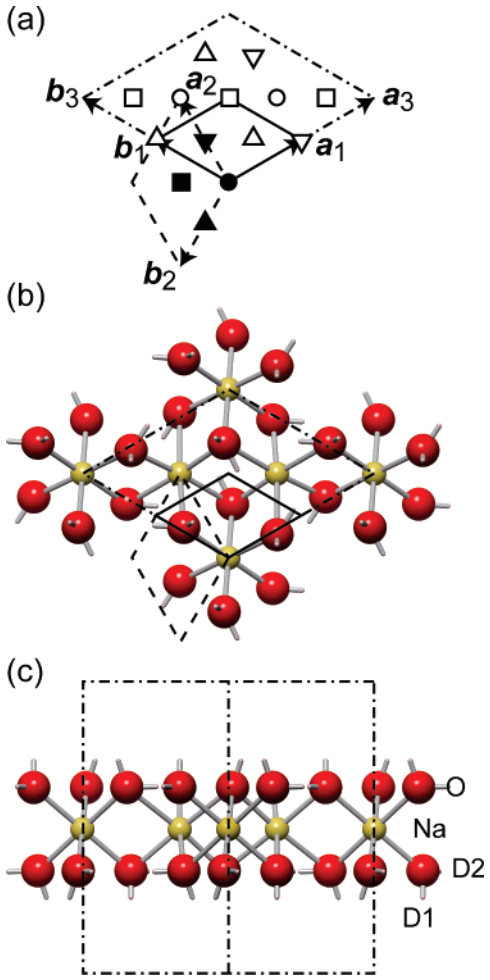

Figure 6. Structure model of the guest basic layer with the $2a \times 2a$ lattice. Dash-dotted lines indicate the $2a \times 2a$ lattice. Endpoints of the shift vectors in the $2/\sqrt{3}a \times 2/\sqrt{3}a$ model are indicated by closed symbols, which were unfolded into their corresponding open symbols in the $2a \times 2a$ model as shown in (a). (b) and (c) are lateral and vertical views of the basic guest layer.

into twelve shift vectors, s'_{ij} ($i = 1-4$, $j = 1-3$) listed in Table 4. For example, $s_1 = 0$ in the $2/\sqrt{3}a \times 2/\sqrt{3}a$ lattice was unfolded into $s'_{1j} = 0$, $2/3a_3 + 1/3b_3$, and $1/3a_3 + 2/3b_3$ in the $2a \times 2a$ lattice, where a_3 and b_3 are lattice vectors for the latter lattice; which correspond to 0, $-b_2$, and a_2, respectively, as shown in Figure 6a. When the guest layers generated by s'_{ij} are denoted as guest′-ij, p(guest′-ij, guest′-ij') will be zero, because p(guest-i, guest-i) were zero as analyzed for the $2/\sqrt{3}a \times 2/\sqrt{3}a$ lattice model. In addition, p(guest′-ij, guest′-$i'j'$) with $i \neq i'$ was set to be equal to each other, i.e., 1/9.

The structure parameters were refined on the basis of this model. The D−O bond length and the D−O−D bond angle were constrained to be 1 Å and 108°, respectively, in the beginning, and the constraints were removed in the final refinement. The final structure parameters are listed in Table 5, and the simulated diffraction pattern is compared with the observed one in Figure 5b. The new structure model with the $2a \times 2a$ guest lattice weakened the 00300 reflection, which resulted in the better agreement between the simulated and the observed patterns, decreasing R_p and R_{wp} from 5.58 and 8.51% to 5.05 and 8.14%, respectively. In addition, the D−O bond lengths and the D−O−D bond angle remained reasonable after the removal of the constraints (0.95 and 0.97 Å for the D1−O2 and D2−O2 bonds, respectively, and 107° for the D−O−D bond angle). The orientation of the D_2O molecules is consistent with those in the previous works[4] and is reasonable. They were oriented to make one of the D atoms face to the negatively charged CoO_2 layer and the O atom face to the positively charged Na^+ ion.

The 2H phase showed a diffuse pattern similar to that of the 3R phase, which suggests that the former has the same guest subsystem as the latter. However, their host subsystems are different, as compared in Figure 7. Two kinds of the host layers were used to form the 2H lattice; one was generated from the other by a symmetry operation of (x, y, $-z$). They were alternatively stacked with a unique shift vector, c_c, to build the host subsystem; the stacking is represented in Table 6. The structure parameters refined using the structure model are listed in the right columns in Table 5. They were very close to those for the 3R phase, suggesting that the 2H and 3R phases have the same crystal structure except for the different stackings of the CoO_2 layers.

Geometric Feature of the Superconductors. The analysis of diffuse bands described above has revealed intralayer ordering of the guests, which have perfect two-dimensional ordering forming a $2a \times 2a$ superlattice. The ordered guest layers are stacked along the c-direction with the short-range interlayer ordering. These aspects have been clarified for the first time by the present study. Further theoretical and experimental approaches are still necessary to know how this guest arrangement affects the electronic structure. However, the electronic and crystal structures are sometimes strongly correlated to each other; for example, a recent theoretical study on the superconductors revealed that magnetic fluctuation strongly depends on the thickness of the CoO_2 layers.[10] Thus it will be worth pointing out the similarities between the guest arrangement and some geometric features of exotic superconductors, e.g., Kagomé lattices and stripes.

When the 3d electrons of the cobalt are assumed to hop through the 2p orbital of the neighboring oxygen, calculation of the hopping matrix reveals that their pathways form four Kagomé lattices hidden in the triangular CoO_2 layer.[11] Their dimensions are $2a \times 2a$, which coincide with the guest lattice

(10) Mochizuki, M.; Ogata, M. *J. Phys. Soc. Jpn.* **2007**, *76*, 013704.
(11) Koshibae, W.; Maekawa, S. *Phys. Rev. Lett.* **2003**, *91*, 257003.

Table 5. Structure Parameters, Fractional Coordinates (*x*, *y*, *z*), and Occupancies (*g*) for the Host and Guest Basic Layers[a]

Host Basic Layer[b]

	3R				2H			
atom	*x*	*y*	*z*	*g*	*x*	*y*	*z*	*g*
Co	0	0	0	1	0	0	0	1
O1	1/3	2/3	0.0986(2)	1	1/3	2/3	0.1013(1)	1

Guest Basic Layer[c]

	3R				2H			
atom	*x*	*y*	*z*	*g*	*x*	*y*	*z*	*g*
Na1	0	0	1/2	1[d]	0	0	1/2	1[d]
Na2	2/3	1/3	1/2	0.200[d]	2/3	1/3	1/2	0.212[d]
O2	0.305(1)	0.9715(2)	0.642(1)	0.893[e]	0.315(1)	0.9818(3)	0.6417(9)	0.893[e]
D1	0.246(1)	0.9133(8)	0.7332(8)	0.929(3)	0.262(1)	0.9274(9)	0.7327(8)	0.927(3)
D2	0.5066(7)	0.0611(6)	0.645(2)	= *g*(D2)	0.5144(8)	0.066(1)	0.603(1)	= *g*(D2)

[a] 3R, $R_p = 5.05\%$ and $R_{wp} = 8.14\%$; 2H, $R_p = 5.75\%$ and $R_{wp} = 9.12\%$. Refined parameters have standard deviations in parentheses. [b] Lattice parameters: for 3R, $a_1 = 2.8238(3)$ Å, $c_c = 9.829(1)$ Å; for 2H, $a_1 = 2.8237(3)$ Å, $c_c = 9.824(1)$ Å. Symmetry operations: x, y, z; $-y, x - y, z$; $-x + y, -x, z$; $-x, -y, -z$; $y, -x + y, -z$; $x - y, x, -z$. [c] Lattice parameters: for 3R, $a_3 = a_1 \times 2$, $c_c = 9.829(1)$ Å; for 2H, $a_3 = a_1 \times 2$, $c_c = 9.824(1)$ Å. Symmetry operations: x, y, z; $-y, x - y, z$; $-x + y, -x, z$; $-x, -y, -z$; $y, -x + y, -z$; $x - y, x, -z$. [d] Na contents were fixed to the analytical values. [e] These occupancies were fixed to the analyzed values.

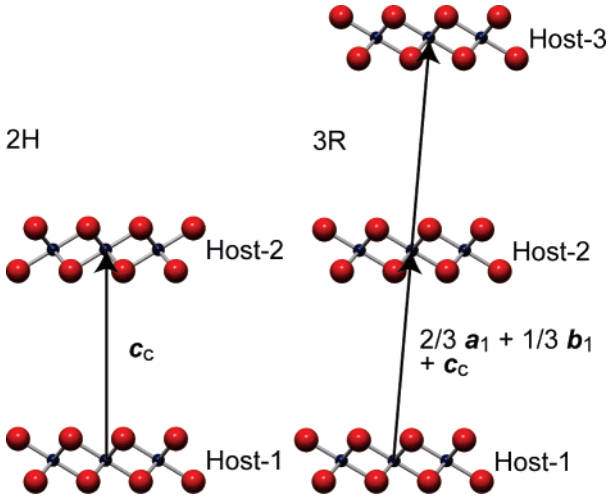

Figure 7. Host subsystems in the 2H (left) and 3R (right) phases.

Table 6. P Table for the Host Subsystem in the 2H Phase

i-th/(*i*+1)-th	host-1	host-2
host-1	0	1
host-2	1	0

used in the present structure refinement. In fact, when the guest layers and the Kagomé lattices are overlapped, they look closely synchronized with each other as shown in Figure 8. On the other hand, by taking into account the guest layer on another side as well, Na^+ ions are aligned one-dimensionally over the CoO_2 layer, whatever pair of the guest layers is selected. They may induce stripes on the CoO_2 layer, which have been proposed as a paradigm to understand high-T_c superconductivity.[12]

Of course, it is unknown whether the guest arrangement plays a dominant role in the superconductivity. However, it will induce structural modulation in the CoO_2 layers, even though the Na^+ ions may be too far away from the CoO_2 layers to affect them as a point charge. The adjacent CoO_2 layers should interact with each other through the interposed

(12) (a) Zaanen, J.; Gunnarsson, O. *Phys. Rev.* **1989**, *B40*, 7391. (b) Emery, V. J.; Kivelson, S. A. *Physica C* **1993**, *209*, 597. (c) Tranquada, J. M.; Buttrey, D. J.; Sachan, V.; Lorenzo, J. E. *Phys. Rev. Lett.* **1994**, *73*, 1003.

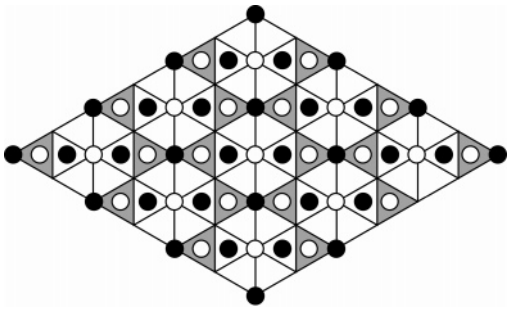

Figure 8. One example of relative positions of the host and guest layers. Among the host and guest layers shown in Figure 3, host-1 layer is interposed between guest-1 and guest-4 layers with overlapping origins. Solid lines indicate the trigonal lattice of the host layer, and the open and closed circles are the positions of the Na^+ ions in the guest-1 and guest-4 layers, respectively. That is, Co atoms are located at the intersections of the solid lines on the $z = 0$ plane, and Na^+ ions are at the positions indicated by the open and closed circles on the $z = -1/2$ and $z = 1/2$ planes, respectively. One of the Kagomé lattices is highlighted by gray.

guest layer; otherwise, the CoO_2 layers will not have a regular stacking sequence to form the 2H or 3R lattices. For instance, a positively charged D atom facing to the CoO_2 layer may attract the negatively charged O atom in the CoO_2 layer to elongate the Co−O bond. This may induce an oscillation in the Co−O bond length or the thickness of the CoO_2 layers in synchronization with the Kagomé lattices or the stripes. They may modulate the electronic structure to some extent, which may split the degenerated four bands originating from the four Kagomé lattices or inhomogenize the charge distribution into a stripe-like pattern. Further structural analysis on the basis of a commensurate model is necessary to determine how the CoO_2 layers are modulated and such a study is now in progress. A theoretical approach is also necessary to know how the modulations influence the superconducting property.

Conclusions

The crystal structures of the two superconducting phases of hydrous sodium cobalt oxides were investigated by neutron powder diffraction. Comparison of their structures showed that the guest arrangement is common to the two phases. The guests are ordered in the interlayer to form a

$2/\sqrt{3}a \times 2/\sqrt{3}a$ trigonal lattice and have short-range ordering along the *c* direction. Only adjacent guest layers over a CoO_2 layer have the following relation: the same guest layers do not adjoin each other.

Acknowledgment. The authors acknowledge Dr. Katsuo Kato for his computer programs. The authors also thank Mr. Satoshi Takenouchi for the inductively coupled plasma atomic emission spectrometry and the redox titration to determine the compositions of the samples.

Supporting Information Available: Figures S1−S3. This material is available free of charge via the Internet at http://pubs.acs.org.

CM0705441